Water Practice & Technology Vol 16 No 3
doi: 10.2166/wpt.2021.039

Comparative study of acid mine drainage using different neutralization methods

Zhong-sheng Huang[a,b,c,*] and Tian-zu Yang[a]

[a] School of Metallurgy and Environment, Central South University, Changsha 410083, Hunan, China

[b] State Key Laboratory of Comprehensive Utilization of Low-Grade Refractory Gold Ores, Xiamen 3361101, Fujian, China

[c] Zijin Mining Group Company Limited, Shanghang 364200, Fujian, China

*Corresponding author. E-mail: ah8225@163.com

Abstract

Two-stage acid mine drainage (AMD) neutralization residue yield is 2.57 t/t acid equivalent using limestone and lime, 15.74% less than the 3.05 t/t acid equivalent yield from single-stage lime neutralization residue. XRD results shows that the main residue component generated by two-stage neutralization is $CaSO_4 \bullet 0.5H_2O$, with a molecular weight 15.70% lower than the $CaSO_4 \bullet 2H_2O$ generated in single-stage neutralization. The differing amount of gypsum crystallization water from the different neutralization processes is the main cause of the different residue yields. While the actual removal rate and pH of Fe^{3+} are consistent with the theory, those for Zn^{2+}, Cu^{2+} and Al^{3+} are inconsistent with the theoretical values, the error rate increasing with increasing pH. Co-precipitation with and adsorption by $Fe(OH)_3$, mainly generated during neutralization, are the main reasons for the difference. The cost of two-stage neutralization is 16.60% less than that of single-stage neutralization when the initial reaction pH is 3.4, but the unit cost begins to increase if the initial reaction pH is raised above 3.4. When the initial pH is 4.0, the cost of two-stage neutralization exceeds that of single-stage neutralization by 4.07%.

Key words: acid mine drainage, comparative study, lime, limestone, single-stage neutralization, two-stage neutralization

Highlights

- Two-stage neutralization residue yield is 15.74% less than single-stage.
- Different crystallization water amount in gypsum caused different neutralization residue yield.
- The co-precipitation adsorption of $Fe(OH)_3$ is the main reason that causes the Zn^{2+}, Cu^{2+} and Al^{3+} actual removal rates to be higher than theoretical.
- The cost of the two-stage neutralization is at a minimum when the initial pH is 3.4.

INTRODUCTION

Acid mine drainage (AMD) is a major challenge to the mining industry due to its environmental consequences. The main cause of AMD is oxidation of sulfide mineral ores, initially exposed by mining activities; for example, through open-pit mining areas, waste rock disposal, and so on. The components of AMD differ (Torres & Auleda 2013) depending on the mine's geological conditions and the metal minerals present. Pyrite is one of the main sources of AMD due to its relative ease of

Water Practice & Technology Vol 16 No 3
doi: 10.2166/wpt.2021.039

oxidization (Kefeni *et al.* 2017). AMD is produced by both active and closed mines (Johnson & Hallberg 2005; Le Pape *et al.* 2017), and AMD yield usually increases sharply during mine development.

Treatment processes differ according to AMD chemical composition and purpose. Neutralization is a traditional and widely used method in treating AMD (Kumar *et al.* 2008; Romero *et al.* 2011; Zheng *et al.* 2011; Alakangas *et al.* 2013; Akinwekomi *et al.* 2017, 2020; Masindi *et al.* 2019). In this process, calcium hydroxide, limestone, sodium hydroxide or alkaline tailings are commonly used as neutralization reagents. The metal and sulfate ions are removed from the AMD as metal hydroxide and gypsum residues, respectively (Tolonen *et al.* 2014). The water is then recycled or discharged, and the solid residue discharged to tailings. Sulfide precipitation is usually used to recover metal ions such as Cu^{2+}, Zn^{2+}, etc. from AMD and Na_2S, NaHS, H_2S, and so on, are the reagents normally used (Chen *et al.* 2014; Luo *et al.* 2017). Ion exchange (Luo *et al.* 2017) and adsorption (Mohan & Chander 2006; Groudev *et al.* 2008; Freitas *et al.* 2011; Zhang 2011) have also been studied widely in treating low concentration AMD. Sulfate-reducing bacteria (SRB) (Foucher *et al.* 2001; Sun *et al.* 2020) use sulfate as a terminal electron acceptor, SO_4^{2-} being converted into H_2S, and then H_2S-selective recovery of some metals, such as copper and zinc, as pure sulfides. SRBs are seldom used because of their low efficiency and high cost.

No matter which AMD treatment process is used, a neutralization process must be used to raise the water's pH above 7.0, using alkaline reagents, before discharge. The price of limestone in China is just one-third that of lime so, to reduce AMD treatment costs, two-stage neutralization by limestone and lime instead of single-stage lime neutralization is valuable. However, neutralization of AMD by these two methods is seldom compared. In this work, residue composition and yield, removal rate, reagent consumption and cost by these neutralization methods are compared.

MATERIALS AND METHODS

Materials

AMD came from one of the Zijin Mining Group mines in China – its average content is shown in Table 1.

Table 1 | Average concentrations found in AMD

Component	Cu^{2+}	Fe^{3+}	H_2SO_4	Zn^{2+}	Al^{3+}
Concentration	85.37 mg/L	8.19 g/L	12.12 g/L	295.64 mg/L	2.07 g/L

The effective calcium oxide and calcium carbonate contents of lime are 75.67% and 11.90%, respectively, and the calcium carbonate content is 96.23% in limestone – Table 2. The average particle sizes were 150 and 74 μm. The XRD traces for lime and limestone are shown in Figure 1. Calcium oxide is the main component of lime – Figure 1(a) – with small amounts of calcium hydroxide, calcium carbonate and quartz. Calcium carbonate is the main component of limestone (Figure 1(b)).

Table 2 | Components in limestone and lime

	Effective CaO	Si	Mg	Al	Fe	$CaCO_3$	Size
Limestone (%)	n/a	0.96	0.97	0.62	0.15	96.23	74 μm
Lime (%)	75.67	2.47	2.15	0.35	0.15	11.90	150 μm

Water Practice & Technology Vol 16 No 3
doi: 10.2166/wpt.2021.039

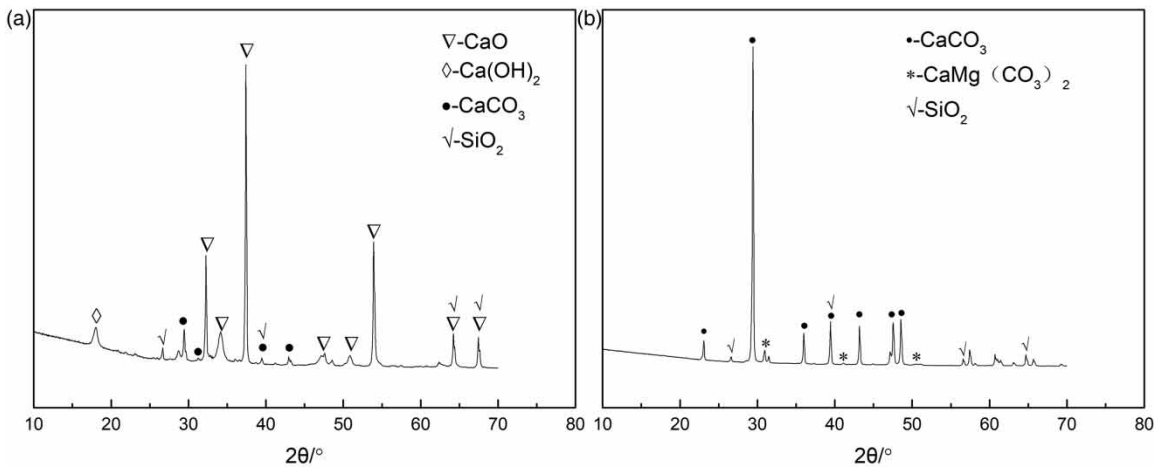

Figure 1 | XRD traces for lime (a) and limestone (b).

Experimental procedure

The tests were carried out in a 400 m^3/h process chain. Figure 2 comprises the flowcharts for (a) the single-stage neutralization process using lime and (b) two-stage neutralization using lime and limestone.

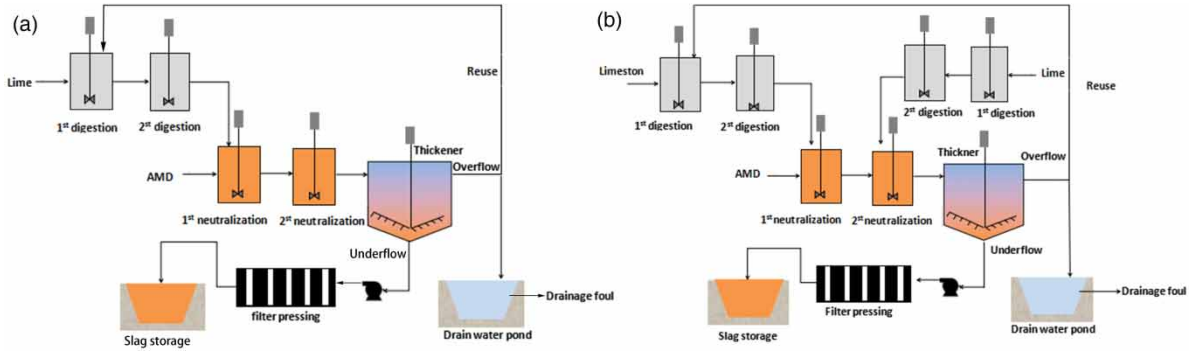

Figure 2 | Neutralization flowcharts – (a) single-stage (b) two-stage.

Single-stage (lime) neutralization: 10% (w/w) lime was added in the first and second reaction tanks, and the pH was controlled at 4.5 and 7.0 in them, respectively. The slurry from the second neutralization tank was thickened and the underflow pumped to the plate-frame pressure filter. Following pressure filtration, the residue was discharged to the tailings pile and the overflow discharged or reused after the pH reached 7.0.

Two-stage neutralization: AMD was pumped continuously into the first neutralization tank and neutralized using 10% (w/w) limestone. The slurry from here flowed automatically to the second neutralization tank, where it was reacted with 10% lime. The slurry from the second neutralization tank flowed to the thickener and the underflow was pumped to the plate-frame pressure filter. The pressure-filter residue was discharged to the tailings pile, and the overflow discharged or reused after the pH reached 7.0.

Analytical methods

Liquid and slurry samples were collected on-line continuously. Wet residue was dried at 50 °C for 8 hours before chemical analysis. Liquid and dry residue elements were analyzed by atomic absorption spectrometry (AAS, iCE3400, Thermo Fisher, USA). The phase composition of the neutralization

Water Practice & Technology Vol 16 No 3
doi: 10.2166/wpt.2021.039

residue was analyzed by X-ray diffraction (XRD) (X'Pert Powder-DY3624, PAN Analytical, Netherlands), scanning electron microscopy (Quanta 650, FEI, USA) and energy spectrum analyzer (EDAX APOLLO Xjime USA).

RESULTS AND DISCUSSION

Theoretical precipitation pH

Two-stage neutralization theoretical precipitation pH: the sulfuric acid in the AMD was neutralized with limestone, and a hydrolytic precipitation process of the Cu^{2+}, Fe^{3+}, Al^{3+} and Zn^{2+} present began as the pH increased gradually. In the second neutralization tank, the slurry pH was further increased to 7.0 after continuous lime neutralization. The limestone/H_2SO_4 neutralization reaction is shown in Formula (1), and the solubility product constants arising for each ion during hydrolysis by formulae (2) to (5) (Ma & Chen 2005).

Single-stage neutralization theoretical precipitation pH: $Ca(OH)_2$ slurry was formed when calcium oxide was digested in water – Formula (6). The sulfuric acid concentration in the AMD decreased and the slurry pH increased gradually as the sulfuric acid was neutralized – Formula (7). Hydrolytic precipitation of the Cu^{2+}, Fe^{3+}, Al^{3+} and Zn^{2+} began at the same time (formulae (2) to (5)).

$$CaCO_3 + H_2SO_4 \rightarrow CaSO_4 \bullet xH_2O + H_2O + CO_2 \uparrow \quad (1)$$

$$Cu^{2+} + 2OH^- \rightarrow Cu(OH)_2 \downarrow K_{sp}^{\theta}(Cu(OH)_2) = [cCu^{2+}] \bullet [c(OH^-)]^2 = 2.2 \times 10^{-20} \quad (2)$$

$$Al^{3+} + 3OH^- \rightarrow Al(OH)_3 \downarrow K_{sp}^{\theta}(Al(OH)_3) = [cAl^{3+}] \bullet [c(OH^-)]^3 = 1.3 \times 10^{-33} \quad (3)$$

$$Fe^{3+} + 3OH^- \rightarrow Fe(OH)_3 \downarrow K_{sp}^{\theta}(Fe(OH)_3) = [cFe^{3+}] \bullet [c(OH^-)]^3 = 4.0 \times 10^{-38} \quad (4)$$

$$Zn^{2+} + 2OH^- \rightarrow Zn(OH)_2 \downarrow K_{sp}^{\theta}(Zn(OH)_2) = [cZn^{2+}] \bullet [c(OH^-)]^2 = 1.2 \times 10^{-17} \quad (5)$$

$$CaO + H_2O \rightarrow Ca(OH)_2 \quad (6)$$

$$Ca(OH)_2 + H_2SO_4 \rightarrow CaSO_4 \downarrow + H_2O \quad (7)$$

Table 3 represents the initial and complete theoretical precipitation pH results for Fe^{3+}, Al^{3+}, Cu^{2+}, Zn^{2+} on the basis of the solubility product constants determined from formulae (2) to (5), the initial AMD ion concentrations (Table 1) and assuming the completed precipitation is 1.0×10^{-5} mol/L.

Table 3 | Calculated initial and complete precipitation pHs

Item	$Cu(OH)_2$ (initial $Cu^{2+} = 1.33 \times 10^{-3}$ mol/L)	$Zn(OH)_2$ (initial $Zn^{2+} = 3.85 \times 10^{-3}$ mol/L)	$Al(OH)_3$ (initial $Al^{3+} = 0.08$ mol/L)	$Fe(OH)_3$ (initial $Fe^{3+} = 0.15$ mol/L)
K_{sp}^{θ}	2.2×10^{-20}	1.2×10^{-17}	1.3×10^{-33}	4.0×10^{-38}
Initial precipitation pH	4.39	6.75	3.40	1.81
Complete precipitation pH	7.0	8.66	4.70	3.20

Theoretical reagent consumption by equivalent acid

The concentration of the various ions in the AMD varied during the trials – see Figure 3 – and it was difficult to calculate limestone and/or lime consumption accurately by AMD volume. To compare reagent consumption, the limestone or lime consumption by Fe^{3+}, Zn^{2+}, Al^{3+}, Cu^{2+} during neutralization hydrolysis was converted into the equivalent consumption of sulfuric acid, using reaction formulae (1) to (7). The results are shown in Table 4.

Water Practice & Technology Vol 16 No 3
doi: 10.2166/wpt.2021.039

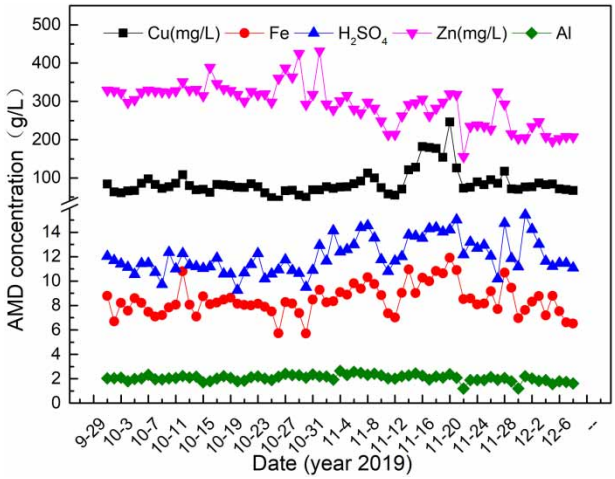

Figure 3 | Ionic concentration variation in the AMD influent.

Table 4 | Equivalent acid neutralization reagent consumption for the metal ions

Equivalence	H_2SO_4	Fe^{3+}	Zn^{2+}	Al^{3+}	Cu^{2+}
Mole	1	1.5	1	1.5	1
Mass	1	2.63	1.50	5.44	1.53

Effect of pH on removal rate

Figure 4 shows the removal rates of H_2SO_4, Fe^{3+}, Al^{3+}, Zn^{2+} and Cu^{2+} increasing as the initial pH of two-stage neutralization increased, while their concentrations decrease.

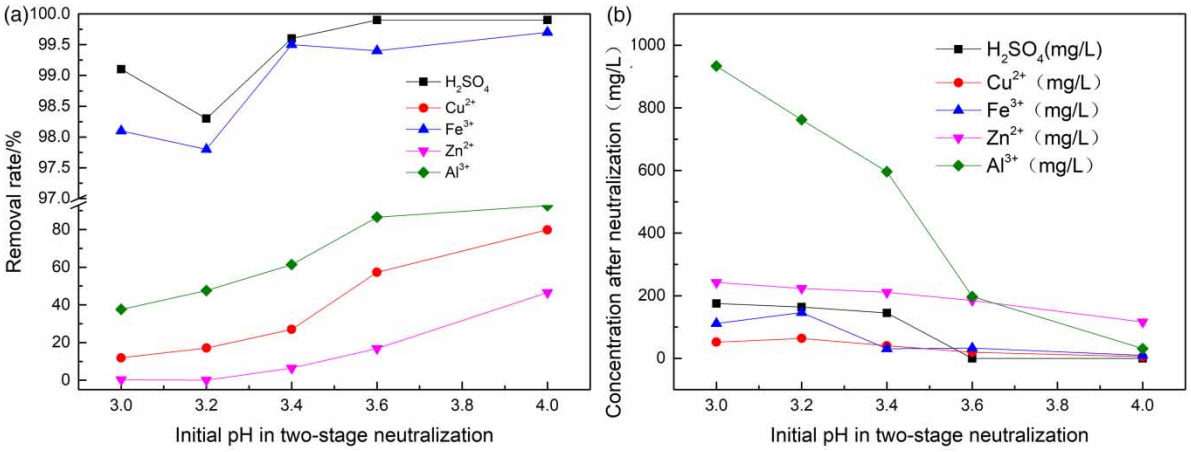

Figure 4 | Effect of initial neutralization pH on removal rate (a) and ionic concentrations after neutralization (b).

Figure 5 shows that the theoretical and actual removal rates of Fe^{3+} were very similar, but the actual Zn^{2+}, Cu^{2+} and Al^{3+} removal rates were much higher than predicted by theory. The difference arises because Fe^{3+} was removed first and precipitated out as $Fe(OH)_3$, as the initial precipitation pH of Fe^{3+} is much lower than those of Al^{3+}, Cu^{2+} and Zn^{2+}. Because of the large specific surface, strong adsorption and negative charge of $Fe(OH)_3$ in the acidic system, the Zn^{2+}, $Cu^{2+}$and Al^{3+} were co-absorbed and co-precipitated into the residue by the $Fe(OH)_3$ generated before reaching

Water Practice & Technology Vol 16 No 3
doi: 10.2166/wpt.2021.039

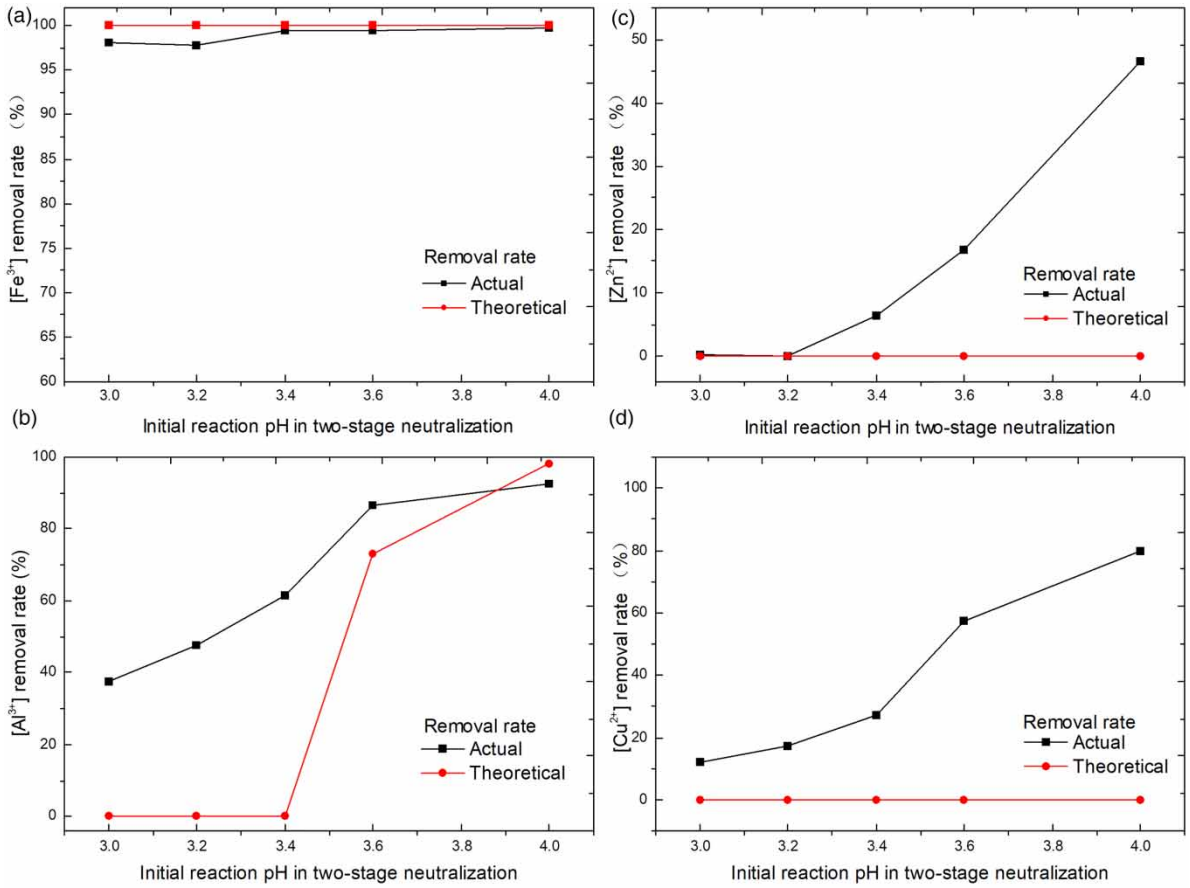

Figure 5 | Effect of pH on actual and theoretical removal rates of Fe^{3+} (a), Al^{3+} (b), Zn^{2+} (c) and Cu^{2+} (d).

their theoretical initial precipitation pHs. As a result, the actual removal rate exceeds the theoretical rate, and the initial precipitation pHs of Zn^{2+}, Cu^{2+} and Al^{3+} were lower than the theoretical values.

Effect of pH on reagent consumption

Normally, limestone consumption increases as the pH increases; however, reagent consumption is higher when the pH is 3.2 than when it is 3.4 or 3.6 (Figure 6(a)) because of the various ionic

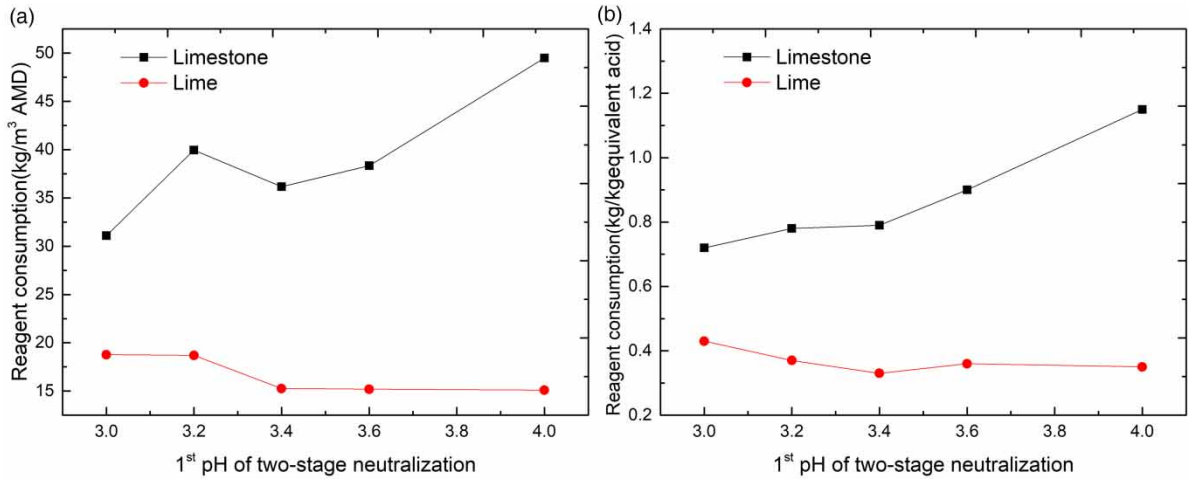

Figure 6 | Reagent consumption by volume of AMD (a) and equivalent acid (b).

Water Practice & Technology Vol 16 No 3
doi: 10.2166/wpt.2021.039

concentrations (see Figure 3). Converting reagent consumption by AMD volume to the acid consumption equivalent shows that limestone consumption increased while lime consumption decreased with increasing pH. The optimal limestone and lime consumptions were determined as 0.79 and 0.33 kg/kg acid equivalent respectively at pH 3.4.

Neutralization residue yield and reaction mechanism

The neutralization residue yield is 2.57 t/t acid equivalent in the two-stage process using limestone and lime, which is 15.74% lower than the 3.05 t/t equivalent from single-stage neutralization using lime (Figure 7). The free water content of the two-stage neutralization residue varied from 42.25% to 42.63% with an average of 42.51%, some 5.84% higher than the 36.67% average free water content of the single-stage neutralization residue (range 35.85% to 37.01%). The residue yield in the limestone and lime, two-stage neutralization is lower than that in the single-stage (lime) neutralization reported by Li (2007), or Ding & Ding (2004), but the mechanism causing the difference in residue yield was not further studied.

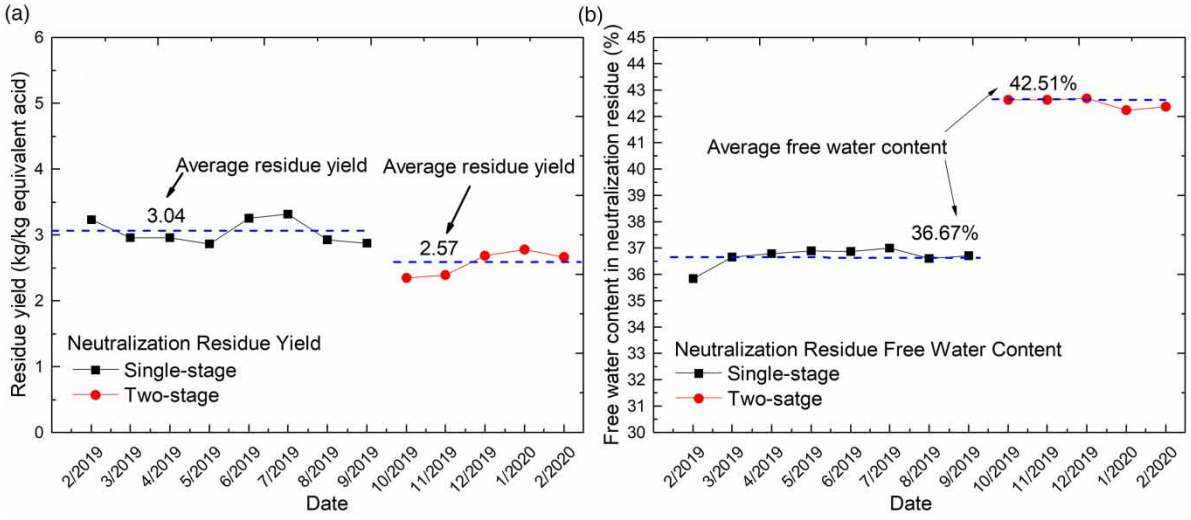

Figure 7 | Yields of (a) neutralization residue and (b) free water in neutralization residue.

Figure 8(a) and 8(c) show that the main residue component from single-stage neutralization is $CaSO_4 \cdot 2H_2O$. The reaction is described in formulae (8) and (9). The residue crystals are fine, which is consistent with the crystal properties of calcium sulfate di-hydrate (Xiang 1998).

Figure 8(b) and 8(d) show that that the main neutralization residue component from two-stage neutralization – limestone and lime – is $CaSO_4 \cdot 0.5H_2O$. The residue's crystal morphology is flaky, irregular, and relatively loose, consisting mostly of secondary particles composed of single, fine grains. This is consistent with the crystal structure of β-$CaSO_4 \cdot 0.5H_2O$ – that is, calcium sulfate hemihydrate (Li 2007). The molecular weight of $CaSO_4 \cdot 0.5H_2O$ is 15.70% less than that of $CaSO_4 \cdot 2H_2O$, consistent with the test results shown in Figure 7(a), which shows that the residue yield from two-stage neutralization is 15.74% lower than that from single-stage neutralization.

It is clear from Figure 5(a) that more than 97% of the sulfuric acid was removed by calcium carbonate in the first reaction during two-stage neutralization. The reaction – see Formula (10) – produced a large amount of CO_2 gas as bubbles, which then cover the $CaSO_4$ crystal surface and prevent contact between it and H_2O.

Water Practice & Technology Vol 16 No 3
doi: 10.2166/wpt.2021.039

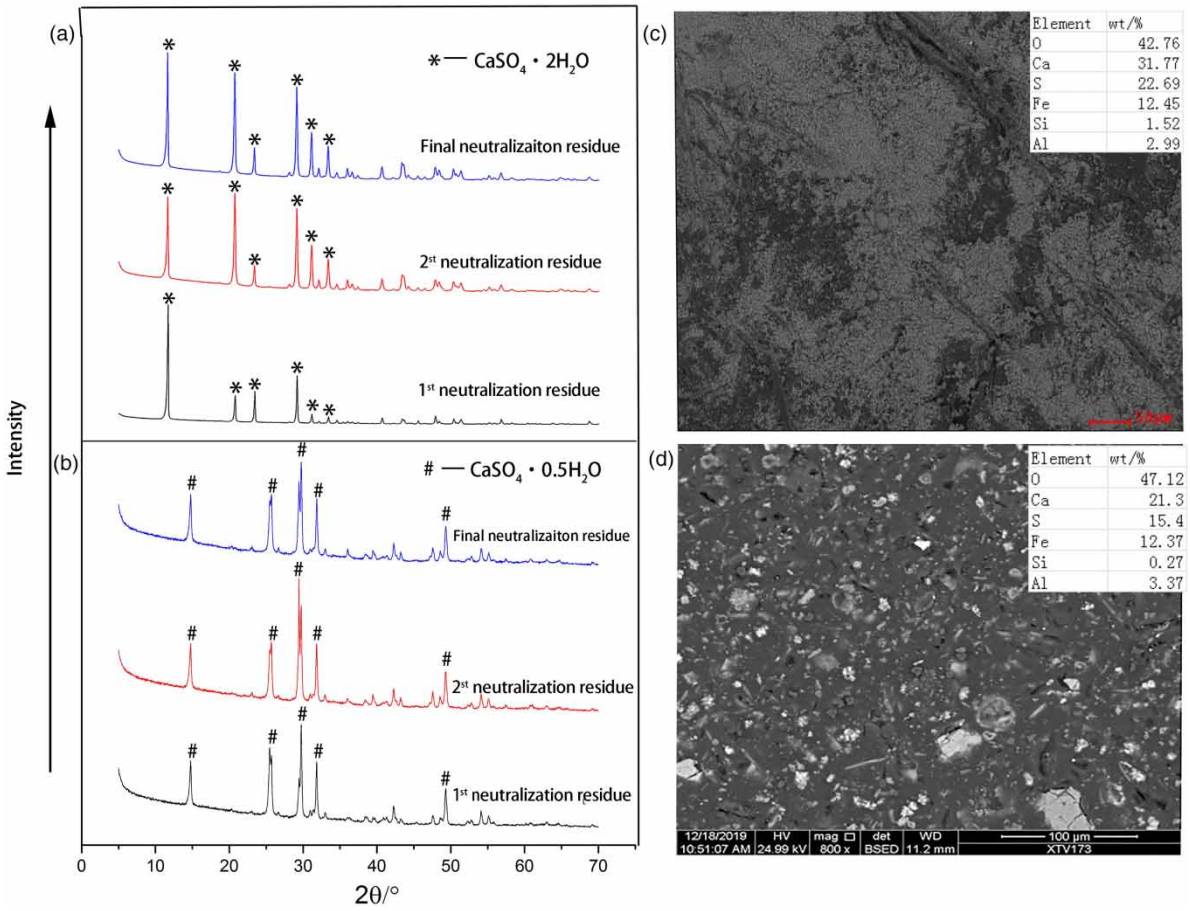

Figure 8 | XRD of (a) single-stage neutralization residue and (b) two-stage neutralization residue, and SEMs of (c) single-stage neutralization residue and (d) two-stage neutralization residue.

In two-stage neutralization, the acidity of the first reaction system exceeds that in single-stage neutralization while the temperature is lower in the first stage. The $CaSO_4$•$0.5H_2O$ reaction mechanism is shown in Formula (11).

$$CaO + H_2O \rightarrow Ca(OH)_2 \downarrow \quad (8)$$

$$Ca(OH)_2 + H_2SO_4 \rightarrow CaSO_4 \bullet 2H_2O \downarrow \quad (9)$$

$$CaCO_3 + H_2SO_4 \rightarrow CaSO_4 + H_2O + CO_2 \uparrow \quad (10)$$

$$CaSO_4 + 0.5H_2O \rightarrow CaSO_4 \bullet 0.5H_2O \downarrow \quad (11)$$

Effect of neutralization methods on cost

Figure 9 shows that the reagent cost of two-stage neutralization falls as the pH increases from 3.0 to 3.4. At pH 3.4, the reagent cost for two-stage neutralization is 0.227 yuan (RMB)/kg equivalent acid (0.035 USD), its lowest level. The reagent cost of single-stage neutralization at pH 3.4 is 16.60% more than that of two-stage neutralization at the same pH. However, two-stage neutralization reagent costs increase as the pH is increased from 3.4 to 4.0. At pH 4.0, two-stage neutralization reagent cost exceeds that of single-stage neutralization, at the same pH, by 4.07%, so the initial reaction pH is the key to achieving cost savings using two-stage neutralization rather than the single-stage process.

Water Practice & Technology Vol 16 No 3
doi: 10.2166/wpt.2021.039

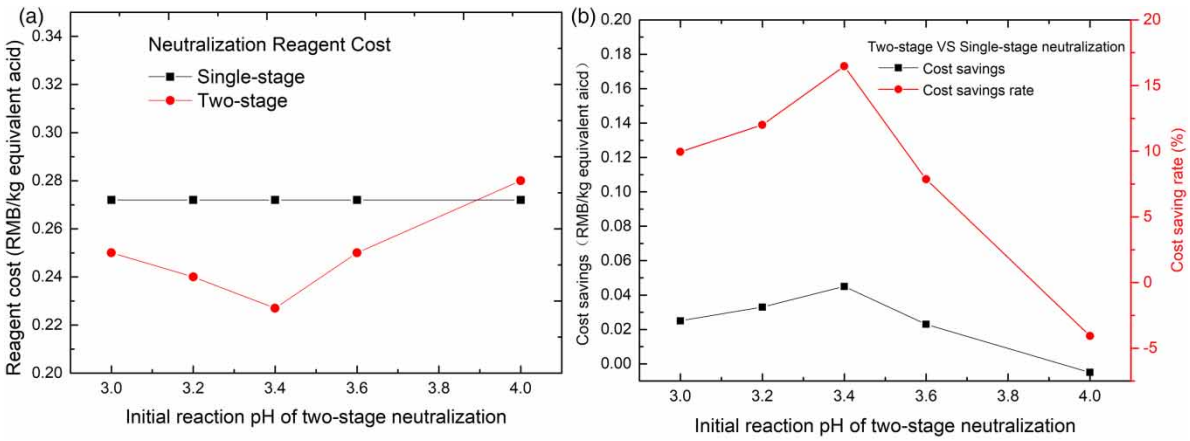

Figure 9 | Reagent cost for different neutralization methods (a) and cost saving by different neutralization methods (b).

CONCLUSIONS

(1) During AMD neutralization using limestone and lime, the theoretical and actual removal rates of Fe^{3+} were basically similar, but the actual removal rates of Zn^{2+}, Cu^{2+} and Al^{3+} were much higher than theoretical predictions. This arose because Fe^{3+} was removed first and precipitated as $Fe(OH)_3$, and, due to its large specific surface, strong adsorption and negative charge in the acidic system, the Zn^{2+}, $Cu^{2+}$and Al^{3+} were co-absorbed and co-precipitated before reaching their theoretical initial precipitation pHs.

(2) The XRD results show that the main components in two-stage and single-stage neutralization residues are $CaSO_4{\cdot}0.5H_2O$ and $CaSO_4{\cdot}2H_2O$, respectively. The molecular weight of $CaSO_4{\cdot}0.5H_2O$ is 15.70% lower than that of $CaSO_4{\cdot}2H_2O$. The different crystalline water content in the gypsum produced by the different neutralization methods caused the residue yield from two-stage neutralization to be 15.74% less than that from single-stage neutralization.

(3) The limestone and lime consumptions were 0.79 and 0.33 kg/kg acid equivalent respectively. When the initial reaction pH is 3.4, the reagent cost is 16.60% less in two-stage than single-stage neutralization, but the saving rate begins to decrease when the initial reaction pH exceeds 3.4. The cost of two-stage neutralization is 4.07% higher than single-stage neutralization when the initial reaction pH is 4.0.

ACKNOWLEDGEMENTS

The research was supported by the Natural Science Foundation of China (No. 51874101). Special thanks to Zijin Mining Group Co., Ltd and the State Key Laboratory of Comprehensive Utilization of Low-Grade Refractory Gold Ore.

DATA AVAILABILITY STATEMENT

Data available within the article or its supplementary materials.

REFERENCES

Akinwekomi, V., Maree, J. P., Zvinowanda, C. & Masindi, V. 2017 Synthesis of magnetite from iron-rich mine water using sodium carbonate. *Journal of Environmental Chemical Engineering* **5**, 2699–2707. https://doi.org/10.1016/j.jece.2017.05.025.

Water Practice & Technology Vol 16 No 3
doi: 10.2166/wpt.2021.039

Akinwekomi, V., Maree, J. P., Masindi, V., Zvinowanda, C., Osman, M. S., Foteinis, S., Mpenyana-Monyatsi, L. & Chatzisymeong, E. 2020 Beneficiation of acid mine drainage (AMD): a viable option for the synthesis of goethite, hematite, magnetite, and gypsum – gearing towards a circular economy concept. *Minerals Engineering* **148**, 1–9. https://doi.org/10.1016/j.mineng.2020.106204.

Alakangas, L., Andersson, E. & Mueller, S. 2013 Neutralization/prevention of acid rock drainage using mixtures of alkaline by-products and sulfidic mine wastes. *Environment Science and Pollution Research* **20**, 7907–7916. https://doi.org/10.1007/s11356-013-1838-z.

Chen, M., Cai, Z., Xiong, L., Cai, Q. & Xu, H. 2014 Experimental study on zinc precipitation by potential regulation-sulfide precipitation. *Nonferrous Metals Science and Engineering* **3**(5), 81–85. https://doi:10.13264/j.cnki.ysjskx.2014.03.015.

Ding, X. & Ding, C. 2004 Treatment of AMD by two-stage neutralization using Limestone and Lime. *Energy Environmental Protection* **18**(2), 27–29.

Foucher, S., Battaglia-Brunet, F., Ignatiadis, I. & Morin, D. 2001 Treatment by sulfate-reducing bacteria of Chessy acid-mine drainage and metals recovery. *Chemical Engineering Science* **56**, 1639–1645. https://doi.org/10.1016/S0009-2509(00)00392-4.

Freitas, A. P. P., Schneider, I. A. H. & Schwartzbold, A. 2011 Bio-sorption of heavy metals by algal communities in water streams affected by the acid mine drainage in the coal mining region of Santa Catarina state. *Minerals Engineering* **24**, 1215–1218. https://doi.org/10.1016/j.mineng.2011.04.013.

Groudev, S., Georgiev, P., Spasova, I. & Nicolova, M. 2008 Bioremediation of acid mine drainage in a uranium deposit. *Hydrometallurgy* **94**, 93–99. https://doi.org/10.1016/j.hydromet.2008.05.023.

Johnson, D. B. & Hallberg, K. B. 2005 Acid mine drainage remediation options: a review. *Science of the Total Environment* **338**, 3–14. https://doi.org/10.1016/j.scitotenv.2004.09.002.

Kefeni, K. K., Msagati, T. & Mamba, B. B. 2017 Acid mine drainage: prevention, treatment options, and resource recovery: a review. *Journal of Cleaner Production* **151**, 475–493. https://doi.org/10.1016/j.jclepro.2017.03.082.

Kumar, V., Klink, M. J., Etchebers, O., Petrik, L. F., Gitari, W., White, R. A., Key, D. & Iwuoha, E. 2008 Neutralization of acid mine drainage using fly ash, and strength development of the resulting solid residues. *South Africa Journal Science* **104**, 317–322.

Le Pape, P., Battaglia-Brunet, F., Parmentier, M., Joulian, C., Gassaud, C., Fernandez-Rojo, L., Guigner, J. M., Ikogou, M., Stetten, L., Olivi, L., Casiot, C. & Morin, G. 2017 Complete removal of arsenic and zinc from a heavily contaminated acid mine drainage via an indigenous SRB consortium. *Journal of Hazardous Material* **321**, 764–772. https://doi.org/10.1016/j.jhazmat.2016.09.060.

Li, X. 2007 Experimental and feasibility study on AMD from processing plant by two-stage neutralization using limestone and lime. *Xinjiang Non-Ferrous Metal* **30**(4), 42–44.

Luo, X., Zhang, X., Wang, T. & Zhang, R. 2017 Study on the application of sulphurization in the treatment of acid waste water containing copper in Zijinshan mountain. *Mining & Metallurgy* **26**(4), 81–83. doi:10.3969/j.issn.1005-7854.2017.04.019.

Ma, L. & Chen, H. 2005 *Basic Chemistry*. Chemistry Industry Press, Beijing, China, pp. 462–463.

Masindi, V., Osman, M. S. & Shingwenyana, R. 2019 Valorization of acid mine drainage (AMD): a simplified approach to reclaim drinking water and synthesize valuable minerals – pilot study. *Journal of Environmental Chemical Engineering* **7**, 1–12. https://doi.org/10.1016/j.jece.2019.103082.

Mohan, D. & Chander, S. 2006 Removal and recovery of metal ions from acid mine drainage using lignite – a low cost sorbent. *Journal of Hazardous Materials* **137**, 1545–1553. https://doi.org/10.1016/j.jhazmat.2006.04.053.

Romero, F. M., Núñez, L., Gutiérrez, M. E., Armienta, M. A. & Ceniceros-Gómez, A. E. 2011 Evaluation of the potential of indigenous calcareous shale for neutralization and removal of arsenic and heavy metals from acid mine drainage in the Taxco mining area Mexico. *Archives of Environmental Contamination and Toxicology* **60**, 191–203. https://doi.org/10.1007/s00244-010-9544-z.

Sun, R., Li, Y., Lin, N., Ou, C., Wang, X., Zhang, L. & Jiang, F. 2020 Removal of heavy metals using a novel sulfidogenic AMD treatment system with sulfur reduction: configuration, performance, critical parameters and economic analysis. *Environment International* **136**, 1–9. https://doi: 10.1016/j.envint.2019.105457.

Tolonen, E. T., Sarpola, A., Hu, T., Ramo, J. & Lassi, U. 2014 Acid mine drainage treatment using by-products from quicklime manufacturing as neutralization chemicals. *Chemosphere* **117**, 419–424. https://doi.org/10.1016/j.chemosphere.2014.07.090.

Torres, E. & Auleda, M. 2013 A sequential extraction procedure for sediments affected by acid mine drainage. *Journal of Geochem Exploration* **128**, 35–41. https://doi.org/10.1016/j.gexplo.2013.01.012.

Xiang, C. 1998 *Building Gypsum and its Products*. China Building Materials Industry Press, Beijing, China, pp. 31–33.

Zhang, M. 2011 Adsorption study of Pb(II), Cu(II) and Zn(II) from simulated acid mine drainage using dairy manure compost. *Chemical Engineering Journal* **172**, 361–368. https://doi.org/10.1016/j.cej.2011.06.017.

Zheng, Y., Peng, Y. & Li, C. 2011 Treatment of acid main drainage by two stage neutralization. *Journal of Central South University (Science and Technology)* **5**(42), 1215–1219. doi:10.3724/SP.J.1011.2011.00468.

First received 6 March 2021; accepted in revised form 18 April 2021. Available online 4 May 2021